MATHEMATICAL MODEL OF TWO-DOF FIVE LINKS CLOSED-CHAIN MECHANISM (PANTOGRAPH)

Abdel Ghany Mohamed[a] , Mohamed Sallam[b] , Mohamed Shamseldin [c]*****, Laylaa EL-Tehewy[d]

[a] Higher Engineering Institute, Thebes Academy, Cairo, Egypt, (on leave from Helwan University), ghanyghany@hotmail.com
[b] Mechatronics Engineering Department, Faculty of Engineering, Egyptian-Chinese University (on leave from Helwan University), eng_sallam@hotmail.com
[c] Mechanical Engineering, Faculty of Engineering, Future University in Egypt, mohamed.abelbbar@fue.edu.eg
[d] Mechatronics Engineering Department, Faculty of Engineering, MTI University, Cairo, Egypt, laylaa.mahmoud@eng.mti.edu.eg
***Corresponding author*: Email address**: mohamed.abelbbar@fue.edu.eg

ABSTRACT

Parallel manipulators have been developed largely for applications that need high accuracy and speed, which make them useful in important fields. This paper presents a detailed mathematical model for a closed chain pantograph mechanism. This task was done by defining its differential equation of motion and implements it using the Matlab Simulink. The mathematical model describes the forward and inverse kinematics, in addition, the dynamic behavior. The mathematical model advantage is studying the parameters variation using different advanced control techniques. This model can be implemented using the Simscape model, which considers a black-box model. To validate the proposed mathematical model for the pantograph, the corresponding model mechanism using the Simscape had been implemented. A comparative study was executed between the mathematical model and the outputs of the Simscape. The results indicated a perfect match for output extracted from Simscape and Simulink. This is evidence for the validity of the inferred equations and Simulink model.

KEYWORDS: Pantograph Modeling; Close Chain Mechanism; Simscape, Matlab Simulink.

1 INTRODUCTION

Parallel robots have become a necessary part of general robots both in academia and in the industry [1]. Besides, with the rapid development of parallel robots, the research on mechanism theory, mobility analysis, dimensional synthesis, kinematics and dynamics modeling [2], and design optimization have been increasing on a large scale.

Fig.1: Five Bar Planar (Pantograph)

The development of parallel robotics and controllable mechanism, a five-bar planar mechanism has become widely used as a mechanical design, which is called a pantograph mechanism shown in **Fig. 1**. The name pantograph refers to the five-sided links used. Four of the five links are moving platform and the fifth one is base platform. The Five bar planar manipulator is a relatively simple mechanism has two degree-of-freedom (DOF) and its kinematics is explicit [3] [4] [5]. However, its characteristics are high speed, high accuracy, low inertia and carrying more weights [6]. For these reasons, it draws a lot of researchers' attention. Some prototypes and commercial products were made, such as 'double SCARA' RP-AH series offered by Mitsubishi Electrics, and DexTAR, five-bar planar manipulator designed by ETS. The five-links planar of the pantograph, which is a simple two degree of freedom (DOF) mechanism (**Fig. 2**), one of them (L0) is passive and the other four links (L1, L2, L3, L4) are active. The system contains only five rotational joints (figure 2). Links 1 and 4 are the driving links. With the help of the appropriate rotation of

Fig.2: Two-DOF Mechanism.

the actuating links, the characteristic point e of the system can follow the desired planar trajectory in the borders of the working zone [7]. Especially, the need for exactly adaptive automation in varied applications has led to higher requirements for operational accuracy and cycle time with robots [8]. Examples of such needs are higher precision assembly, faster product handling, surface finishing, better measurements, surface finishing, and milling capabilities [9]. Additionally, there is a high demand for off-line programming to eliminate touch-up of programmed positions; in other words, robots must perform their task with better load capacity and accuracy in operations. A general trend of meeting these requirements is to make use of
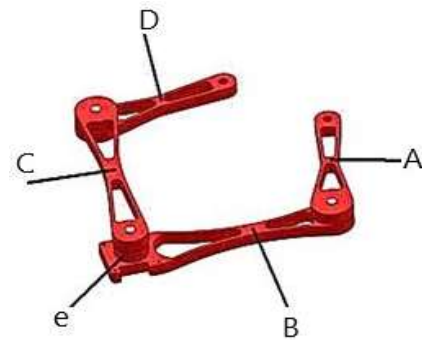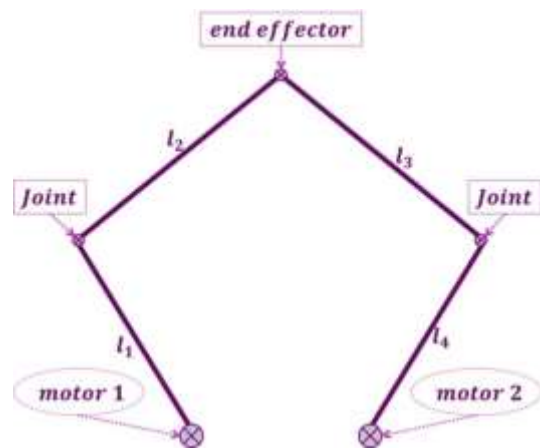
parallel robots, which have excellent potential capabilities, including high rigidity, high accuracy, and high loading capacities [10].

This paper is organized as following: Forward Kinematics as the first section, followed by Investors Kinematics, then Dynamics including Velocity vectors, and then Kinetic Energy, which will lead us to the equations of movement and in the end the results part. This paper features a complete infer of all the mathematical equations that represent the pantograph in addition to the saturation portion detailed in Section 6 in addition to simulations on Simulink Matlab and also on Simscape and comparing results. A number of researchers have previously provided a portion of the mathematical equations that represent the pantograph, such as [11] [12].

2   DIRECT KINEMATICS

The constrain of the five-link mechanisms as shown in **Fig. 3** is given by

$$l_1 \bar{a}_1 + l_2 \bar{b}_1 - l_3 \bar{c}_1 - l_4 \bar{d}_1 - l_5 \bar{n}_1 = 0 \qquad [11]\square \qquad (1)$$

Where l_i for i=1,….., 5 is the length of links , $(\bar{a}_1, \bar{b}_1, \bar{c}_1, \bar{d}_1, \bar{n}_1)$ are unit vectors. The relation between the task space $(X = (x_e \ \ y_e)^T)$ and joint space $(\theta = (\theta_1 \ \theta_2 \ \theta_3 \ \theta_4)^T$ of the five-link mechanism system can be calculated, where x and y are the Cartesian coordinates of Joint e with
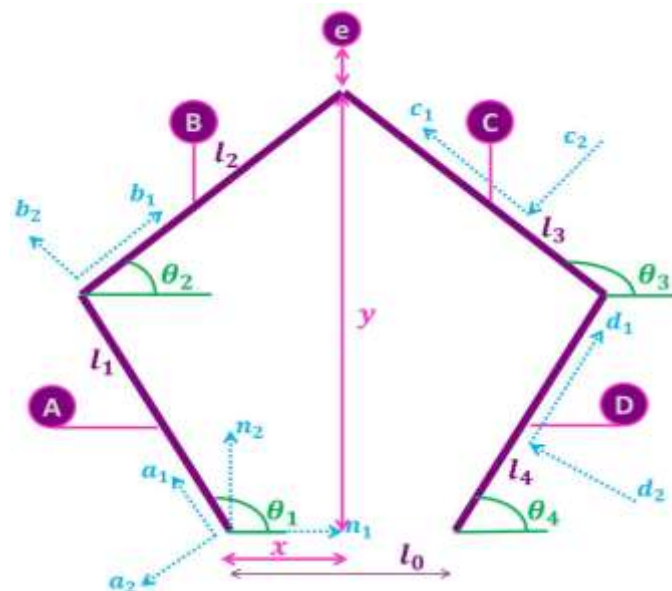
respect to the plane (n_1, n_2) of reference [13], as shown in **fig. 3** [14].

In order to solve for x and y using θ_1 and θ_4 , define the following vector:

$$r^{oe} = x\bar{n}_1 + y\bar{n}_2$$

$$= l_1\bar{a}_1 + l_2\bar{b}_1$$

$$= l_1\left(\cos\theta_1\ \bar{n}_{1+}\sin\theta_1\ \bar{n}_2\right) + l_2(\cos\theta_2\bar{n}_1 + \sin\ \theta_2\ \bar{n}_2)$$

$$= l_1(\cos\theta_1 + \cos\theta_2)\bar{n}_1 + l_2(\sin\theta_1 + \sin\ \theta_2\ )\bar{n}_2 \qquad (2)$$

Where r^{oe} is the position vector of point e in the plane $(n_1\,,n_2)$ by using equation 2, obtain the following two scalar equations

Fig. 3 : Direct Kinematics Mechanism.

$$x_e = l_1\cos\theta_1 + l_2\cos\theta_2 \qquad (3)$$

$$y_e = l_1\sin\theta_1 + l_2\sin\ \theta_2 \qquad (4)$$

Equations (3) and (4) can simulate the forward kinematics of the five-link mechanism. Need to solve θ_2 in terms of θ_1 by the holonomic constraints. Where θ_2 is passive angle and has to be described using the active angle of the device (θ_1 and θ_4). From equation (1) can conclude that:

$$l_1\cos\theta_1\ \bar{n}_{1+}\sin\theta_1\ \bar{n}_2) + l_2(\cos\theta_2\bar{n}_1 + \sin\ \theta_2\ \bar{n}_2) - l_3(\cos\theta_3\ \bar{n}_{1+}\sin\theta_3\ \bar{n}_2) -$$
$$l_4(\cos\theta_4\bar{n}_1 + \sin\ \theta_4\ \bar{n}_2) - l_5\bar{n}_1 = 0 \qquad (5)$$

Equation (5) gives the following:

$$l_1\cos\theta_1 + l_2\cos\theta_2 - l_3\cos\theta_3 - l_4\cos\theta_4 - l_5 = 0 \qquad (6)$$

$$l_1\sin\theta_1 + l_2\sin\ \theta_2 - l_3\sin\theta_3 - l_4\sin\ \theta_4 = 0 \qquad (7)$$

Thus, from equations (6 and 7) can deduce x_e which expresses the X coordinate of the point and y_e is Y coordinate as following

$$x_e = l_1\cos\theta_1 + l_2\cos\theta_2 = l_3\cos\theta_3 + l_4\cos\theta_4 + l_5 \qquad (8)$$

$$y_e = l_1\sin\theta_1 + l_2\sin\ \theta_2 = l_3\sin\theta_3 + l_4\sin\ \theta_4 \qquad (9)$$

The Newton-Raphson theory or Trigonometry method can be used to find θ_3 and θ_2. In this work, the trigonometry method was used to calculate it.

From equation (8) and (9), θ_1 and θ_4 are independent. So, θ_3 and θ_2 consider as a function of θ_1 and θ_4:

$$\theta_3 = 2\tan^{-1}\left(\frac{A \pm \sqrt{A^2 + B^2 - C^2}}{B - C}\right)$$

(10)

Where,

$$A = 2l_3 l_4 \sin\theta_4 - 2l_1 l_3 \cos\theta_1$$

$$B = 2l_3 l_5 - 2l_1 l_3 \cos\theta_1 + 2l_4 l_3 \cos\theta_4$$

$$C = l_1^2 - l_2^2 + l_3^2 + l_4^2 + l_5^2 - l_1 l_4 \sin\theta_1 \sin\theta_4 - 2l_1 l_5 \cos\theta_1 - 2l_4 l_5 \cos\theta_4 - 2l_4 l_1 \cos\theta_4 \cos\theta_1$$

From equations (9) and (10) will result that,

$$\theta_2 = \sin^{-1}\left[\frac{l_3 \sin\theta_3 + l_4 \sin\theta_4 - l_1 \sin\theta_1}{l_2}\right]$$

(11)

3 INVERSE KINEMATICS

By added the equations (8) and (9) and remove the passive angles θ_2 and θ_3 and can get direct relation between the coordinates of the end-effector and link lengths to the actuating angles θ_1 and θ_4 as following equations [15].

$$\theta_1 = 2\tan^{-1}\left(\frac{-E \pm \sqrt{D^2 + E^2 - F^2}}{-D - F}\right)$$

(12)

Where,

$$D = x_e$$

$$E = y_e$$

$$F = \frac{l_1^2 - l_2^2 + x_e^2 + y_e^2}{2l_1}$$

$$\theta_4 = 2 \tan^{-1}\left(\frac{-H \pm \sqrt{G^2 + H^2 - I^2}}{-G - I}\right) \tag{13}$$

Where,

$$G = x_e - l_5$$

$$H = y_e$$

$$I = \frac{l_4{}^2 + l_5{}^2 - l_3{}^2 - 2x_c l_5 + x_e{}^2 + y_e{}^2}{2l_4}$$

The links lengths are constant for the robot, which helps to easily solve the above equations. From equation (12) and (13) it can obtained θ_1 and θ_4 without known θ_2 and θ_3. The only inputs need for controlling the five-link mechanism is the location of the end-effector (x_e and y_e).

4 DYNAMUCS SOLUTION:

The position vector of the center of mass of link A with respect to reference plane (n_1, n_2) is given by:

$$^0r^{A_0} = \frac{l_1}{2}\bar{n}_1 = \frac{l_1}{2}\cos\theta_1\,\bar{n}_1 + \frac{l_1}{2}\sin\theta_1\,\bar{n}_2 \tag{14}$$

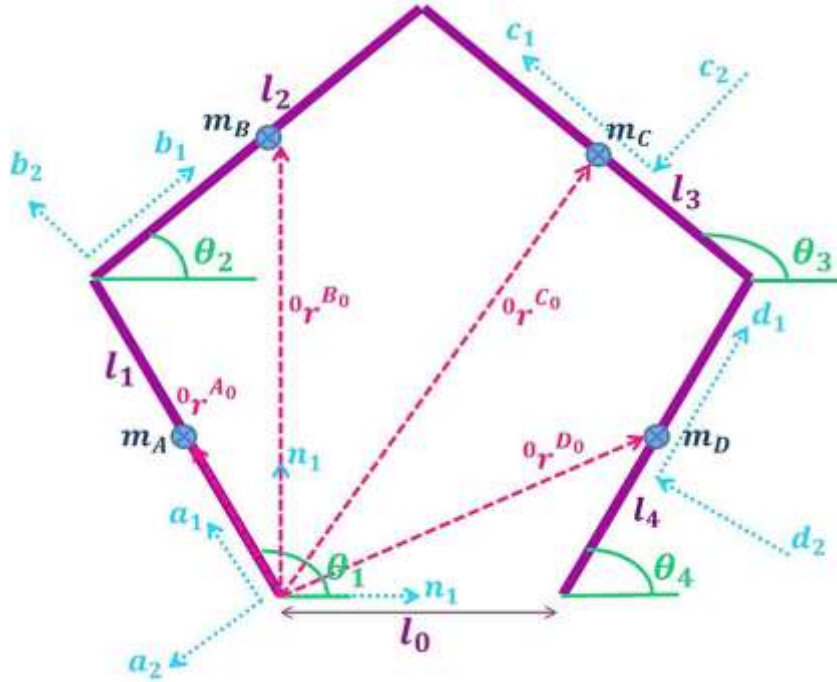The position vector of the center of mass of link B is given by:

$$^0r^{B_0} = l_1\bar{n}_1 + \frac{l_1}{2}\bar{n}_1 = l_1\cos\theta_1\,\bar{n}_1 + l_1\sin\theta_1\,\bar{n}_2 + \frac{l_2}{2}\cos\theta_2\,\bar{n}_1 + \frac{l_2}{2}\sin\theta_2\,\bar{n}_2$$
$$= \left(l_1\cos\theta_1 + \frac{l_2}{2}\cos\theta_2\right)\bar{n}_1 + \left(l_1\sin\theta_1 + \frac{l_2}{2}\sin\theta_2\right)\bar{n}_2 \tag{15}$$

Similarly, the position vector of the center of mass of link D is given by:

$$^0r^{D_0} = l_0\bar{n}_1 + \frac{l_4}{2}\bar{d}_1 = l_0\bar{n}_1 + \frac{l_4}{2}(\cos\theta_4\bar{n}_1 + \sin\theta_4\,\bar{n}_2)$$
$$= \left(l_0 + \frac{l_4}{2}\cos\theta_4\right)\bar{n}_1 + \left(\frac{l_4}{2}\sin\theta_4\right)\bar{n}_2 \tag{16}$$

Finally, the position vector of the center of mass of link C is given by:

Fig. 4 : Velocity Vectors.

$$^0_r{}^{C_0} = l_0\bar{n}_1 + l_4\bar{d}_1 + \frac{l_3}{2}\bar{c}_1$$
$$= l_0\bar{n}_1 + l_4\cos\theta_4\bar{n}_1 + l_4\sin\theta_4\,\bar{n}_2 + \frac{l_3}{2}\cos\theta_3\,\bar{n}_1 + \frac{l_3}{2}\sin\theta_3\bar{n}_2$$
$$= \left(l_0 + l_4\cos\theta_4 + \frac{l_3}{2}\cos\theta_3\right)\bar{n}_1 + \left(l_4\sin\theta_4 + \frac{l_3}{2}\sin\theta_3\right)\bar{n}_2 \qquad (17)$$

5 The velocity vector of the calculated position vectors with respect to the plane (n_1, n_2):

Velocity vector of the center of mass of link A in the plane of reference (n_1, n_2) (**Fig. 4**):

$$^N V^{A_0} = -\frac{l_1}{2}\dot{\theta}_1\sin\theta_1\,\bar{n}_1 + \frac{l_1}{2}\dot{\theta}_1\cos\theta_1\,\bar{n}_2 \qquad (18)$$

Velocity vector of the center of mass of link B:

$$^N V^{B_0} = -\left(l_1\,\dot{\theta}_1\,\sin\theta_1 + \frac{l_2}{2}\dot{\theta}_2\sin\theta_2\right)\bar{n}_1 + \left(l_1\,\dot{\theta}_1\,\cos\theta_1 + \frac{l_2}{2}\dot{\theta}_2\cos\theta_2\right)\bar{n}_2 \qquad (19)$$

Velocity vector of the center of mass of link D is:

$$^N V^{D_0} = -\left(\frac{l_4}{2}\dot{\theta}_4\sin\theta_4\right)\bar{n}_1 + \left(\frac{l_4}{2}\dot{\theta}_4\cos\theta_4\right)\bar{n}_2 \qquad (20)$$

Velocity vector of the center of mass of link C is:

$$^N V^{C_0} = -(l_4 \dot{\theta}_4 \sin \theta_4 + \frac{l_3}{2} \dot{\theta}_3 \sin \theta_3) \bar{n}_1 + (l_4 \dot{\theta}_4 \cos \theta_4 + \frac{l_3}{2} \dot{\theta}_3 \cos \theta_3) \bar{n}_2 \qquad (21)$$

6 KINETIC ENERGY (K):

Links A and D has a rotational motion only so its kinetic energy is:

$$K_A = \frac{1}{2} \frac{m_A l_1^{\,2}}{3} \dot{\theta}_1^{\,2} \qquad (22)$$

$$K_D = \frac{1}{2} \frac{m_D l_4^{\,2}}{3} \dot{\theta}_4^2 \qquad (23)$$

But Links B and C have a rational and translation motion so its kinetic energy is:

$$K_B = \frac{1}{2} I_B \dot{\theta}_2^{\,2} + \frac{1}{2} m_B (^N V^{B_0})^2 = \frac{1}{2} \frac{m_B l_2^{\,2}}{12} \dot{\theta}_2^{\,2} + \frac{1}{2} m_B (^N V^{B_0})^2$$
$$= \frac{1}{2} \frac{m_B l_2^{\,2}}{12} \dot{\theta}_2^{\,2} + \frac{1}{2} m_B \left(l_1^{\,2} \dot{\theta}_1^{\,2} + \frac{l_2^{\,2}}{4} \dot{\theta}_2^{\,2} + \frac{l_1 l_2}{2} \dot{\theta}_1 \dot{\theta}_2 \cos(\theta_1 - \theta_2) \right) \qquad (24)$$

$$K_C = \frac{1}{2} I_C \dot{\theta}_3^{\,2} + \frac{1}{2} m_C (^N V^{C_0})^2 = \frac{1}{2} \frac{m_C l_3^{\,2}}{12} \dot{\theta}_3^{\,2} + \frac{1}{2} m_C (^N V^{C_0})^2$$
$$= \frac{1}{2} \frac{m_C l_3^{\,2}}{12} \dot{\theta}_3^{\,2} + \frac{1}{2} m_C \left(l_4^{\,2} \dot{\theta}_4^{\,2} + \frac{l_3^{\,2}}{4} \dot{\theta}_3^{\,2} + \frac{l_3 l_4}{2} \dot{\theta}_3 \dot{\theta}_4 \cos(\theta_3 - \theta_4) \right) \qquad (25)$$

Total kinetic energy:

$$L = K_A + K_B + K_C + K_D \qquad (26)$$

Equation of motion by Lagrangian equation [16]:

$$T = Torque = \frac{\partial}{\partial t} \frac{\partial L}{\partial \dot{\theta}_i} - \frac{\partial L}{\partial \theta_i}$$

By using Lagrangian equation obtain by torque, T1 and T2, Where (m, w, v) are constants.

$$T_1 = \left(m_{11} \ddot{\theta}_1 + m_{12} \ddot{\theta}_4 + w_1 \dot{\theta}_1 + w_2 \dot{\theta}_4 \right) - \left(w_3 \dot{\theta}_1^{\,2} + w_4 \dot{\theta}_4^{\,2} + w_5 \dot{\theta}_1 \dot{\theta}_4 \right) \qquad (27)$$

$$T_2 = \left(m_{21} \ddot{\theta}_1 + m_{22} \ddot{\theta}_4 + v_1 \dot{\theta}_1 + v_2 \dot{\theta}_4 \right) - \left(v_3 \dot{\theta}_1^{\,2} + v_4 \dot{\theta}_4^{\,2} + v_5 \dot{\theta}_1 \dot{\theta}_4 \right) \qquad (28)$$

7 EQUATION OF MOTION:

$$T = J(q)\ddot{\theta} + C(\theta, \dot{\theta}) + g(\theta) \qquad [17]$$

Because the pantograph is planar system, thus $g(q)$ was neglected.

$$T_1 = A_1\ddot{\theta}_1 + B_1\ddot{\theta}_4 + C_1(\dot{\theta}_1\dot{\theta}_4) \qquad (29)$$

$$T_2 = A_2\ddot{\theta}_1 + B_2\ddot{\theta}_4 + C_2(\dot{\theta}_1\dot{\theta}_4) \qquad (30)$$

From equation (29) and (30), as a matrix form, where A and B are the inertia matrix [18]

$$\begin{bmatrix} T^1 \\ T_2 \end{bmatrix} = \begin{bmatrix} A_1 & B_1 \\ A_2 & B_2 \end{bmatrix} \begin{bmatrix} \ddot{\theta}_1 \\ \ddot{\theta}_4 \end{bmatrix} + \begin{bmatrix} C_1(\dot{\theta}_1\dot{\theta}_4) \\ C_2(\dot{\theta}_1\dot{\theta}_4) \end{bmatrix} \qquad (31)$$

$$\begin{bmatrix} \ddot{\theta}_1 \\ \ddot{\theta}_4 \end{bmatrix} = \begin{bmatrix} A_1 & B_1 \\ A_2 & B_2 \end{bmatrix}^{-1} \left[\begin{bmatrix} T^1 \\ T_2 \end{bmatrix} - \begin{bmatrix} C_1(\dot{\theta}_1\dot{\theta}_4) \\ C_2(\dot{\theta}_1\dot{\theta}_4) \end{bmatrix} \right] \qquad (32)$$

1. BOUNDARY CONDITIONS:

It is an important part which is the permissible boundary for a mechanism, so that the link does not reach the singularity state during the path [19].

For this to be achieved Q_5 must not be equal to 180 degrees but rather greater.

So, $Q_5 < 180$ shown in **fig. 5**

$$Q_5 = 540 - (180 + \theta_1) - (180 - \theta_4 + \theta_3) - (180 + \theta_1 - \theta_2) - (\theta_4) \qquad (33)$$

So the first boundary:

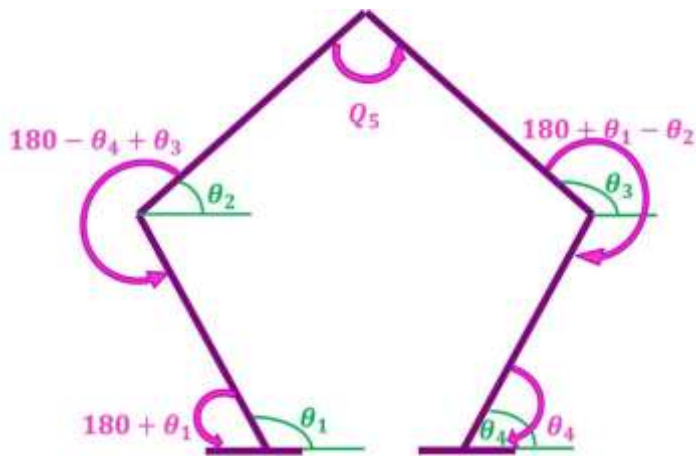$$Q_5 = (\theta_2 - \theta_3) < 180 \qquad (34)$$
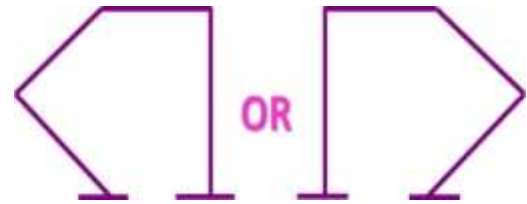
Fig. 5 : First Boundary Condition.

Fig. 6 : Second and Third Conditions.

Second one: In order for the mechanism not to reach the position shown in **Fig. 6**, θ_2 must be greater than θ_1.

Third one: θ_4 must be greater than θ_3.

$$(\theta_2 > \theta_1) \tag{35}$$

$$(\theta_4 > \theta_3) \tag{36}$$

The three rules (35), (36), and (37), can be implemented using the logic gate (AND), as will be explained later in the attached **Fig. 7** and **Fig. 8** in the Result section.

8 RESULTS:

- After applying the equations that were deduced in this paper to the Simulink Matlab program shown in **fig. 7**, then to the Simscape shown in **fig. 8**.
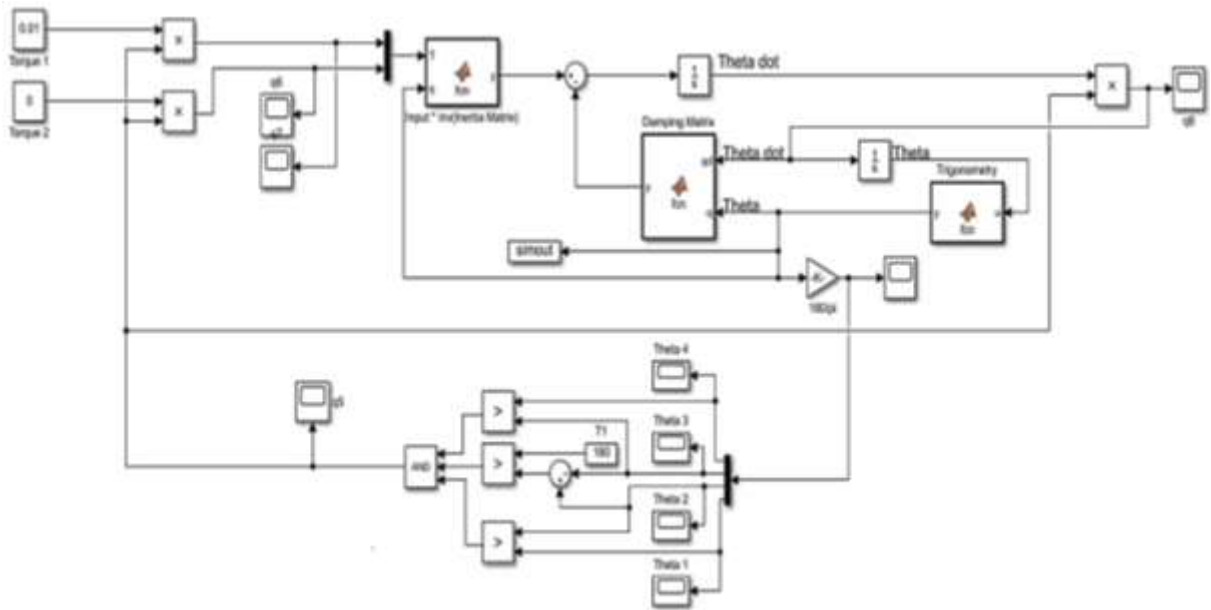
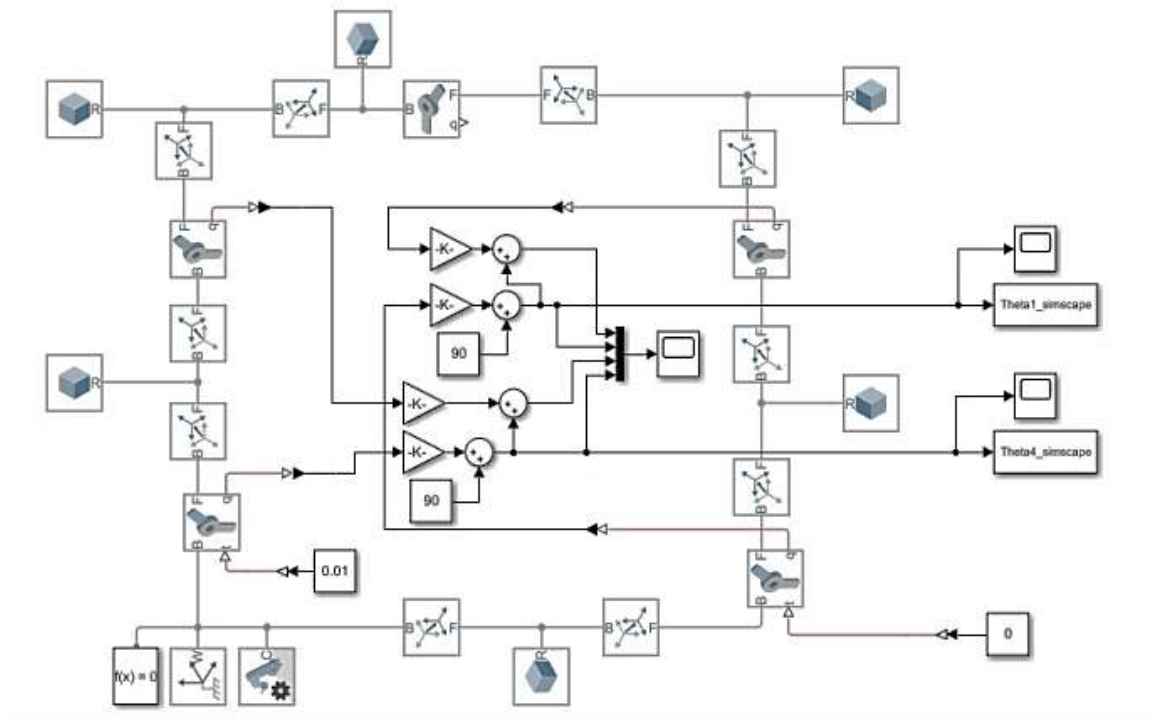**Fig. 7:** Simulink Model of Pantograph Mechanism.

Fig. 8: Simscape Model of Pantograph Mechanism.

- When The input of motor1 torque is: $(T_1 = 0.01)$, and motor2 torque is: $(T_2 = 0)$ Where the previously mentioned three saturation rules are fulfilled, and based on **Table.1** that shows he robot parameters The results of the output were found identical as follows in **Fig.**

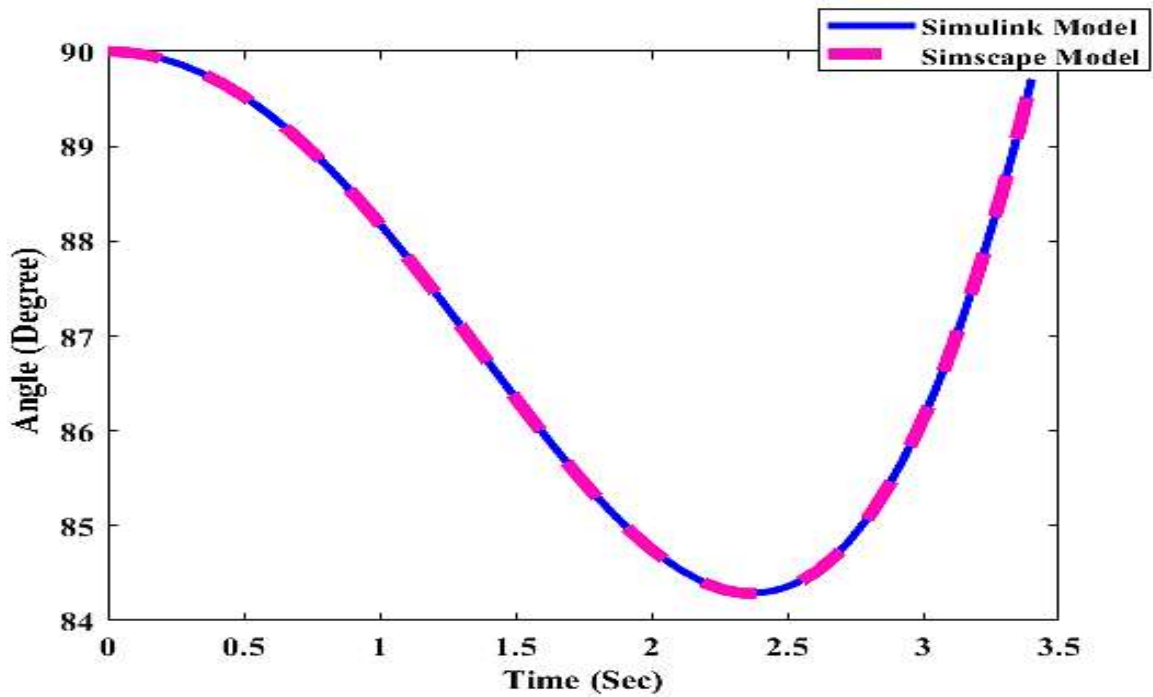**9** and **Fig. 10**. Where the Y-axis expresses the angle in degrees, and the X-axis expresses time in sec :
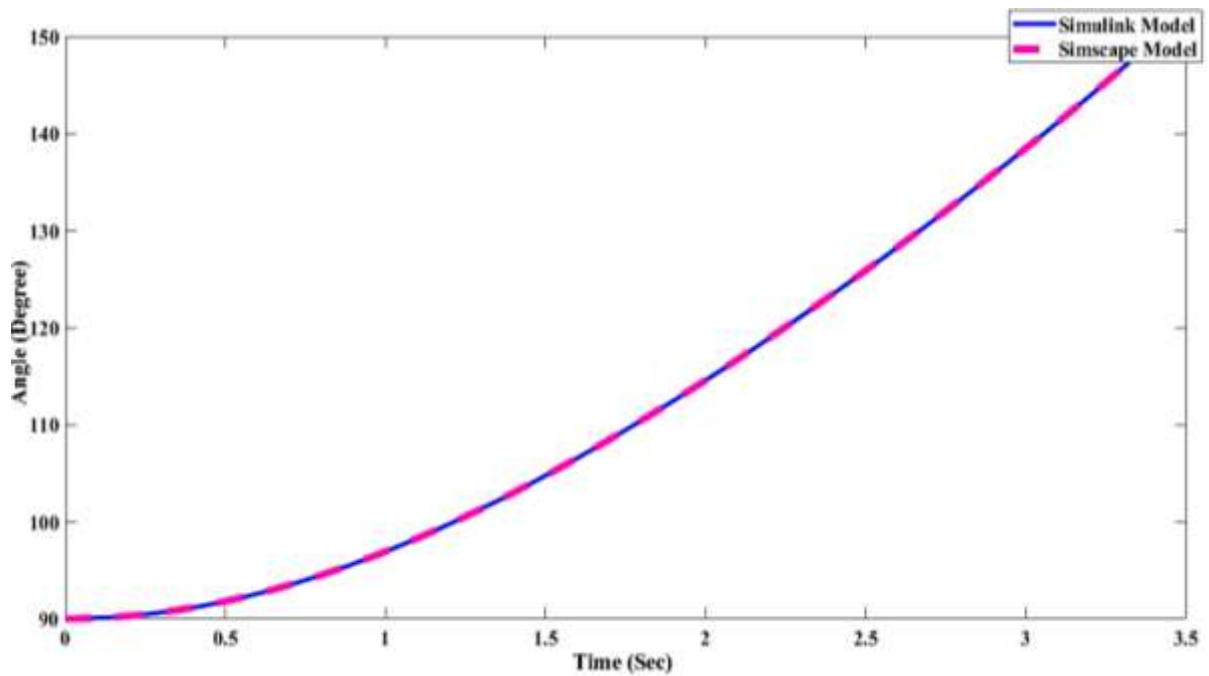

Fig. 9: Theta_1 from Simscape and Simulink.

Fig. 10: Theta_4 from Simscape and Simulink.

Table 1: The Robot Parameters.

Mass of links :	1 of unit mass
Length of links	0.2 unit length

9 CONCLUSION:

- A detailed mathematical model for a closed chain pantograph mechanism has been implemented using the Matlab Simulink. The mathematical model demonstrates the differential equations of the forward kinematics, inverse kinematics, and dynamics. To verify the proposed mathematical model for pantograph, a comparative study was executed between the mathematical model and the outputs of the Simscape. The simulation results show that the both of Simscape and Simulink model are identical. This is evidence for the validity of the inferred equations and the validity of the Simulink model.

- Future work: The Simulink model will be used later to set more than one control and test the efficiency of each of them.

REFERENCES:

1. Patel, Y. D. and George, P. M. (August 2012) . "Parallel Manipulators Applications a Survey," *Jornal of Modern Mechanical Engineering*, (Vol. 2, pp.57-64).

2. Lafmejani, A.S., Masouleh, M.T. and Kalhor, A. (2018) . "Gough-Stewart Parallel Robot Using Backstepping-Sliding Mode Controller and Geometry-Based Quasi Forward Kinematic Method. Robot," *International Conference on System Science and Engineering (ICSSE)*, (Vol. 54, pp.96-114).

3. Zhang, K., Huang ,T. and Wang, C. (2006) . "Kinematics and Dynamics Analysis of a Planar Hybrid Five Bar Actuator," *9th International Conference on Control, Automation, Robotics and Vision (ICARCV) on IEEE,* (pp.1-6).

4. Karnopp, D. and Margolis, D. (1979) . "Analysis and Simulation of Planar Mechanism Systems Using Bond Graphs.," *Journal of Mechanical Design*, (Vol. 101, pp.187-191).

5. He, B., Xu, S., Zhou, Y. and Wang, Z. (2017) . "Mobility Properties Analyses of a Wall Climbing Hexapod Robot," *Journal of Mechanical Science and Technology*, (pp.1333-1344).

6. Wang, Y., Wu, C., Yu, L. and Mei, Y. (March 2018) . "Dynamics of a Rolling Robot of Closed Five-Arc-Shaped-Bar Linkage," *Journal of Mechanism and Machine Theory on ScienceDirect*, (Vol. 121, pp.75-91).

7. Konishi, Y., Aoyama, T. and Inasaki, I. (1988) . "Trajectory Generation and Control of a Five-Bar-Link Parallel Direct-Drive Robot," *Journal of Robotics & Computer-Integrated Manufacturing*, (Vol .4 , pp.395-402).

8. Desai, R. and Muthuswamy, S. (2020) . "A Forward, Inverse Kinematics and Workspace Analysis of 3RPS and 3RPS-R Parallel Manipulators", *Iranian Journal of Science and Technology, Transactions of Mechanical Engineering*, (pp.115-131).

9. Zhao, Q., Guo, J. and Hong, J. (2018) . "Assembly Precision Prediction For Planar Closed-Loop Mechanism In View of Joint Clearance and Redundant Constraint", *Journal of Mechanical Science and Technology* , (Vol. 32, pp.3395-3405).

10. Rahman, L., Carbonari, L., Caldwell, D. and Cannella, F. (2017) . "Kinematic Analysis, Prototypation and Control of a Novel Gripper for Dexterous Applications", *Journal of Intelligent and Robotic Systems* , (Vol. 91, pp.193-206).

11. Khalil, I., Abu Seif, M, "Modeling of a Pantograph Haptic Device",

http://www.mnrlab.com/uploads/7/3/8/3/73833313/modeling-of-pantograph.pdf.

12. Campion, G., Wang, Q. and Hayward, V. (August 2005). "The Pantograph Mk-II: A Haptic Instrument", *International Conference on Intelligent Robots and Systems IEEE/RSJ*, (pp.723-728).

13. Ha, C., Yoon, J., Kim, C., Lee, Y., Kwon, S. and Lee, D. (2018) . "Teleoperation of a Platoon of Distributed Wheeled Mobile Robots With Predictive Display", *Jurnal of Autonomous Robots*, (pp.1819-1836).

14. Farag, R., Badawy, I., Magdy, F., Mahmoud, Z. and Sallam, M. (2020) . "Real-Time Trajectory Control of Potential Drug Carrier Using Pantograph"Experimental Study" ", *International Conference on Advanced Intelligent Systems and Informatics*, (pp.759-768).

15. Bin, Z., Jianbin, C. and Zhencai, Z. (2011) . "Dynamic Simulation of Hybrid-driven Planar Five-bar Parallel Mechanism Based on Sim-Mechanics and Tracking Control", *International Journal of Advanced Robotic Systems*, (pp.28-33).

16. Abou Seif, M., Hassan, A., El-Shaer, H., Misra, S. and Khalil, I. (2017) . "A Magnetic Bilateral Tele-Manipulation System Using Paramagnetic Microparticles for Micromanipulation of Nonmagnetic Objects", *IEEE International Conference on Advanced Intelligent Mechatronics (AIM),* (pp.1095-1102).

17. Sallam, M., Saif, I., Saeed, Z. and Fanni, F. (2020) . "Lyapunov-Based Control of a Teleoperation System in Presence of Time Delay", *International Conference on Advanced Intelligent Systems and Informatics*, (pp.759-768).

18 Shafei, A.M. and Shafei, H.R. (2018) . "Dynamic Modeling of Tree-Type Robotic Systems by Combining 3×3 Rotation and 4×4 Transformation Matrices," *jurnal of Multibody System Dynamics*, (pp.367-395).

19. Francis, P., Eastwood,K. W., Bodani,V., Looi, T., and Drake, J. M. (2018) . "Design, Modelling and Teleoperation of a 2 mm Diameter Compliant Instrument for the da Vinci Platform", *Annals of Biomedical Engineering*, (pp.1437-1449).